Modeling Mechanical Behavior of Nanocrystalline tungsten - Molecular Dynamics Simulation

A.Tahiri[a*], M. Idiri[a], B.Boubeker[a]

Abstract—The mechanisms of deformation in body centered cubic nanocristalline tungsten three dimensions subjected to uniaxial tensile loading is investigated using molecular dynamics simulation. Stress induced the motion of partial dislocation. Twinning boundary and ductile shear fracture were observed in the grain boundaries during the tensile deformation of nanocristalline tungsten. Moreover, the fraction atoms of (fcc + bcc) increases with increasing of the applied strain and such phase transformations were found to be reversible with respect to the applied stress. Also, we found that the average stress over an inelastic stress interval 7%-16% decreases with grain refinement below 9.6 nm, indicating a breakdown in Hall-Petch relation.

Keyword: deformation; nanocristalline tungsten; grain size; partial dislocation; grain boundaries; twinning boundary; phase transformations; Hall-Petch relation; molecular dynamics.

1 INTRODUCTION

Nanocristalline tungsten (nc-W) has better physical and chemical properties than massif tungsten. As a new nonmaterial, it has wider application prospect in aerospace [1], electronic machine [2, 3], bio-pharmaceutical and other fields [1]. Also, many commercial applications such as light bulbs, vacuum tube filaments and electrodes. Tungsten is a refractory metal due to its excellent physical and chemical properties [4]. Such as elastic modulus E, yield strength and fracture strength [5-6]. Uniaxial deformation has become a widely used tool for studied the mechanical behavior of nanocrystalline (nc) metals [7]. Atomistic simulations have been shown to be a powerful tool of studying plasticity behavior and deformation mechanisms for nc materials, particularly their mechanical behavior [8-9]. Up to date a lot of investigators interested to this behavior. Such as Pradeep studied Grain size dependency for nc bcc-Fe using Molecular Dynamic (MD) Simulations, and observed a decrease in the average flow stress of Fe nanocrystalline was found due to the decrease with grain refinement below 13.22 nm. Moreover, this work demonstrated the breakdown in the conventional Hall–Petch relation [10]. Jong studied by MD simulation the effect of grain size on the deformation behavior of nc body-centered cubic iron,and observed this breakdown for the average flow stress in inelastic strain range 4-15% [11]. Many works investigated mechanical properties and plastic deformation mechanisms for bulk nc bcc metals, because of their engineering and technological importance [12, 12, 13, 14].

In this paper we have been studied the mechanical properties, mechanisms of deformation and fraction of atoms as a function the average grain size of nc-W ranging from 7,9nm to 11,5nm using MD simulation and Common neighbor analysis. Further, we have demonstrated the breakdown in the conventional Hall–Petch relation.

- *Abdellah Tahiri ; [(a)] Laboratoire d'Ingénierie et Matériaux (LIMAT), Faculté des Sciences Ben M'Sik, Université Hassan II of Casablanca, Morocco*
  Abl.tahiri@gmail.com
- *Mohamed Idiri ; [(a)] Laboratoire d'Ingénierie et Matériaux (LIMAT), Faculté des Sciences Ben M'Sik, Université Hassan II of Casablanca, Morocco*
  Idiri2010@gmail.com
- *Brahim Boubeker ; [(a)] Laboratoire d'Ingénierie et Matériaux (LIMAT), Faculté des Sciences Ben M'Sik, Université Hassan II of Casablanca, Morocco*
  brahimboubeker@gmail.com

2 SIMULATION METHOD

The MD simulation solves Newton's equations of motion and gives the trajectory of each atom in each time. The forces on an atom are computed as negative gradients of the potential energy of each atom [15]. The source of this potential energy is the interatomic potential, which limits the physics of how atoms interact with each other, and can be considered as the critical component of an MD simulation. An interatomic potential uses the location of an atom relative to all of its neighbors to calculate its potential energy. The mathematical form of an interatomic potential is typically selected and then parameters are determined by fitting to experimental and quantum mechanical simulation data; for this reason, potentials are considered to be empirical [16].The embedded atom method is currently a common technique used in MD computer simulation of metallic systems [17]. The method provides a good description of the interatomic forces in the system, particularly for fcc metals. It calculates the interatomic potentials in metals and models forces between atoms as follows

$$E = \frac{1}{2}\sum_{ij} V(r_{ij}) + \sum_{i} F(\rho_i), \quad \rho_i = \sum_{i \neq j} \varphi(r_{ij}), \quad (1)$$

Where E is the total energy of the system, $V(r_{ij})$ represents the pair interaction energy between an atom i and its neighboring atom j, $\mathbb{V}(r_{ij})$ is the electronic density function, and $F(\rho_i)$ represents an embedding function accounting for the effects of the free electrons in the metal [18]. In particular, we used the Embedded atom model (EAM) potential functions developed in [19]. In this study, MD simulations are performed using the Large Scale Atomic/Molecular Massively Parallel Simulator code (LAMMPS) [20].

In the present paper, atomistic simulations of uniaxial tensile deformation of nc bcc W were performed. All samples the dimensions (20X20X20 nm^3) contained respectively 5, 9, 13 and 16 grains with deferent size. Periodic boundary conditions were used in all three directions. In this configuration the grains is random locations and crystallographic orientations according to the Voronoi construction [21]. The bottom 10 Å of the substrate are wall; and the top of the sample surface was treated as a free surface (fig1). The time step was 1 fs during

the simulations. Before tensile loading, samples were subjected to energy minimization by the conjugate gradient method and annealing at 300 K for 100 ps with a Nose/Hoover isobaric–isothermal (NPT) ensemble. Tensile deformation performed at a strain rate of 10^{-10} s^{-1}. The atomic arrangements of the samples, including dislocations and GBs, were then visualized using a common neighbor analysis tool of OVITO software [22].

.

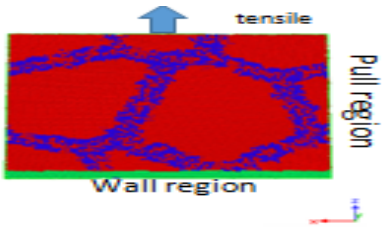

Fig 1 : snapshot of samples present pull region and wall

2.1 results and discution

In this section, we will first describe the simulated results of the mechanical properties of nc W, including the elastic modulus, stress-strain behavior, Hall-petch relationship. Deformation mechanisms of both nc-W will be described and discussed. Secondly we will then discuss, the evolution of phase transformation in GBs W during uniaxial.

2.2 stress-strain behavior

Fig 2 : shows the stress-strain curve of nc-W of the averaging grain size 9.6nm tested at a strain rate of 1.10^{-10} s^{-1}. The elastic modulus along [001] derived from the linear portion of the stress-strain curve is around 401GPa. Zhe chen calculated Young's modulus of nc W for the averaging grain size 5nm using potential embedded H and He and found 311.7GPa [23]. It has been shown that the value of Young modulus elastic moduli is related to the volume fractions of GBs and triple junctions (Tjs) are present in the constructed specimens. The maximum tensile strength of nc-W along [001] is around 18 GPa at a strain of around 16%. This curve does show true plastic region with the strain variation around 7%-16% this phenomenon can be explained by the presence of a set of mechanism of plasticity such as twin boundary formation, dislocation migration and grain boundary sliding.

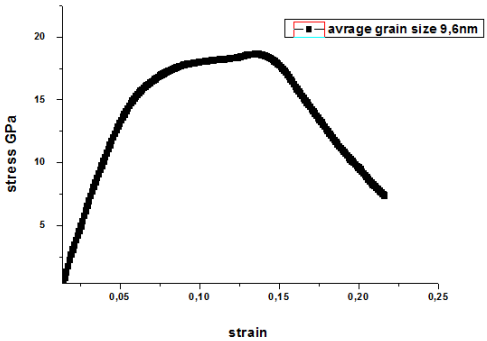

Fig 2 . Stress – strain curve of the tensile deformation nc W. GB model with average size 9.6nm at 300K and $1.10^{-10}s^{-1}$ of strain rate

2.3 Localization the plasticity mechanisms with molecular dynamics simulations

We used MD and OVITO software to analyzed tensile deformation of nc W with grains size ranging from 7.9 nm to 11.5 nm

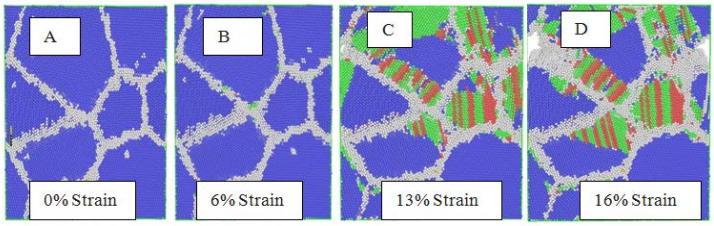

Fig 3 : Snapshot of GB model with 0% to 16% of applied strain

We can see in (fig3-B) the plastic deformations that begin to motion GB at 6% of the applied strain from grain interior. This phenomenon is accentuated when the rate of deformation increases. At 16% of applied strain we clearly observe the ductile shear fracture and twin deformation from grain interior (fig4-a). This deformation twining occurs due to the presence of partial deformation in the grain. This may be due to the phase transition phenomenon from bcc to fcc and hcp. it can also be related to GB sliding [24, 25, 26, 27, 28] and grain rotations [29, 30] and GB migrations [31,32] in nc-W bcc. Van Swygenhoven and Derlet [25] utilized MD to observe grain boundary sliding in fcc metals which was accommodated by atomic shuffling within the GB along with stress-assisted free volume migration.

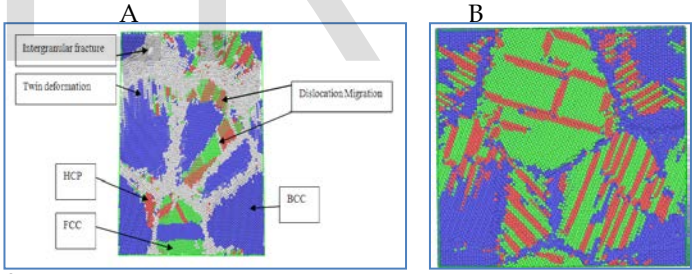

Fig 4: snapshot of GB model with 16% strain. Existence of several phases Body Centered Cubic (bcc), Face Centered Cubic(fcc), Hexagonal close-packed (hcp)

Fig 5-A shows fraction of atoms (fcc+hcp) as a function of tensile strain for various grain sizes of nc W. The fraction of clusters consist of mostly fcc structure and only a small portion of hcp structure, which will be clearly shown in the deformed configuration in Fig 4(B). The appearance of the (fcc +hcp) clusters begins at a applied strain more than 5% for each grain size, which corresponds to the onset of plasticity. After onset of plasticity, the fraction of (fcc + hcp) atoms increases with increased strain. Moreover, a peak fraction (fcc+hcp) exists for each grain size. And the fraction of (fcc+hcp) atoms starts to decrease after attaining the peak value. This peak explained that phase transitions induced by stress in nc W bcc metals that are reversible according to the applied stress [12]. This is reasonable since the fcc and hcp structures are thermodynamically unstable compared with the bcc structure. This explica-

tion is noticed in fig 5(B).

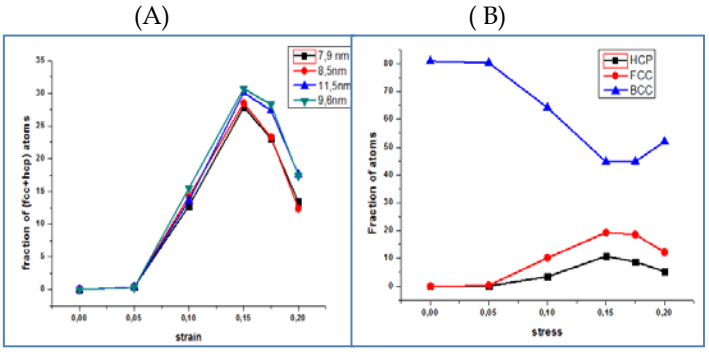

Fig 5. (A). Shows fraction (fcc+ hcp) of vs strain for different average grin size; (B) evolution of fraction atoms as a function of the stress for specimens' with 9.6nm in average grain size.

The averaging grain size depends of the plasticity, thus in fig 6, we show the variation of atom fraction as a function of the average grain size d. We note that the fraction of fcc and hcp increases with increasing of the grain size. A common feature of these mechanisms is that they all represent collective motion of groups of atoms and should alter the internal grain structure of the material. Hasnaoui et al. [33] used MD simulations to observe the emergence of shear planes nc Ni through the alignment of GB planes via grain rotation, GB sliding, and GB migration, which then resulted in localized shear deformation as well as grain coalescence and growth.

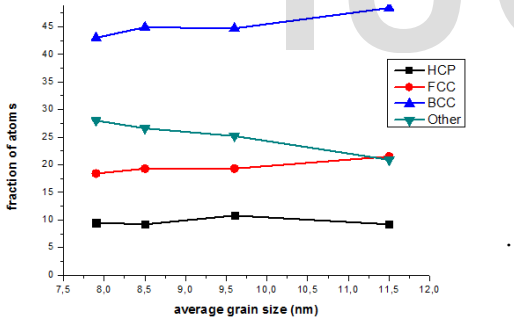

Fig 6 . Fraction of atom fcc and hcp structure vs. averaging grain size at 16% the stress

Fig 7, Shows the evolution the stress acording to the strain for different average grain size ranging from 7.9nm to 11.5nm. We have reported that stress dependent of the average grain size in inelastic region. For gave this observation a signification , we have investigated the average stress over a inelastic stress interval 7%-16% vs. inverse square root of grain size ($d^{-1/2}$) were plotted in fig 8. These average stresses were found to increase to a maximum value of 17.7 GPa with average grain size of 9.5nm, but then to decrease with further grain refinement. Moreover, we observed the conventional Hall-Petch relation for grain size larger the 9.5nm. These observations are consistent with recent observations on other bcc metals with nc [5]

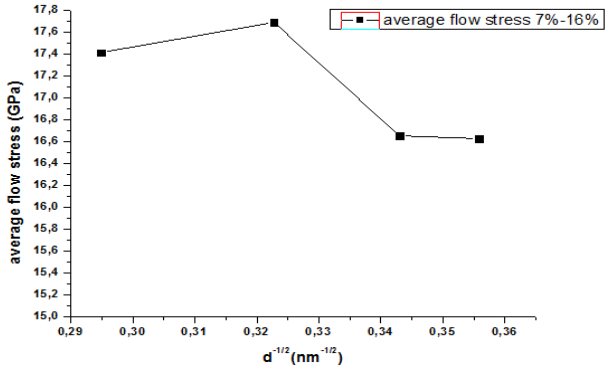

Fig 7. Variation average flow stress (7%-16%) vs. inverse square root of grain size ($d^{-1/2}$)

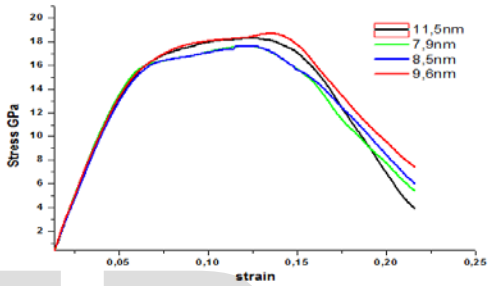

Fig 8. Stress – strain curve of the tensile deformation nc W the average grain size ranging from 7.9 to 11.5 nm at 300K and $1.10^{-10}s^{-1}$

3. Conclusion

In the present work, mechanical properties and deformation mechanisms of nc bcc W under tensile deformation have been studied by MD simulation using EAM potential. The main conclusions are:

- The 401 GPa as value of Young modulus calculated by derived from the linear portion of the stress-strain curve for critical grain size 9.6nm;
- The plastic deformation investigation has shown the presence of several deformation mechanisms as twin formation, dislocation migration and interganular fracture;
- The phase transformation studied during the applied strain, shows that fraction of atom of the fcc and hcp increases with the both increasing of the applied strain and the mean grain size;
- The conventional Hall-Petch relation is breakdown for grain size larger than 9.6 nm;
- We have shown that MD simulations are capable of studied phase transition on GB plasticity, and nanoscale phenomenon of GB strengthening for understanding the mechanical proprieties of nc W.

.

REFERENCES

[1] Bin Ma, Qiuhua Rao, Yuehui He, Molecular dynamics simulation of temperature effect on tensile mechanical properties of single crystal tungsten nanowire, Computational Materials Science 117 (2016).

[2] C. Santato, M. Odziemkowski, M. Ulmann, and J. Augustynski, " Crystallographically oriented mesoporous WO3 films: synthesis, characterization, and applications", J. Am. Chem. Soc., 2001, 123, 10639-10649.

[3] A.G. Umnov Y. Shiratori H. Hiraoka, Giant field amplification in tungsten nanowires, Applied Physics A June 2003, Volume 77, Issue 1, pp 159–161.

[4] E. Lassner, W.D. Schubert, Tungsten: Properties, Chemistry, Technology of the Element, Alloys and Chemical Compounds, Academic/Plenum Publishers, New York, 1998.

[5] S.A Kotrechko, A.V Filatov and A.V. Ovsjannikov, Molecular dynamics simulation of deformation and failureof nanocrystals of bcc metals,Theoretical and Applied Fracture Mechanics 45 (2006) 92–99.

[6] Yuan F P "Atomistic simulation study of tensile deformation in bulk nanocrystalline bcc iron", Sci China Phys MechAstron September (2012) Vol. 55 No. 9.

[7] K.S. Kumar , H. Van Swygenhoven , S. Suresh, Mechanical behavior of nanocrystalline metals and alloys, Acta Materialia 51 (2003) 5743–5774.

[8] R Komanduri, N. Chandrasekarana, and L.M Rao,. "Molecular dynamics (MD) simulation of uniaxial tension of some single-crystal cubic metals at nanolevel" International Journal of Mechanical Science 43(2001)2237-2260.

[9] Li J, Ngan A H W, Gumbsch P. Atomistic modeling of mechanical behavior. Acta Mater, 2003, 51: 5711–5742.

[10] Pradeep Dungriyal, S.P. Singh, Rajesh Prasad, Grain size Dependency, Plasticity and Dynamic Property Evaluation for Nano-crystalline BCC-Fe using Molecular Dynamic Simulations, Procedia Engineering 173 (2017) 1975 – 1982.

[11] Jong Bae Jeon, Byeong-Joo Lee, and Young Won Chang, Molecular dynamics simulation study of the effect of grain sizeon the deformation behavior of nanocrystalline body-centeredcubic iron, ScriptaMaterialia 64 (2011) 494–497.

[12] Pan Z L, Li Y L, Wei Q. Tensile properties of nanocrystalline tantalum from molecular dynamics simulations. Acta Mater, 2008,;56:3470.

[13] Tahiri A, Idiri M, Boubeker B (2018) Molecular Dynamics Studies of Temperature and Grain Size Effects on Mechanical Properties of Nanocrystalline Tungsten. J Nanomater Mol Nanotechnol 7:1.

[14] A.Tahiri, M. Idiri, S. El joumani, B.Boubeker, Nano-indentation of Nanocrystalline Tungsten – A Molecular Dynamic Simulation, RRJOMS , Volume 6, Issue 1, March, 2018.

[15] Lesar R. "Introduction to Computational Materials Science". Cambridge University Press, (28 mars 2013).

[16] Tadmor E. & Miller R. Modeling Materials. Cambridge University Press, 2011.

[17] Daw M.S., Baskes M.I, 1984. "Embedded-atom method – derivation and application to impurities, surfaces, and other defects in metals". Physical Review B 29 (12), 6443–6453.

[18] Finnis M., 2003. Interatomic Forces in Condensed Matter. Oxford University Press, pp. 129–186.

[19] J. Wang, Y.L. Zhou, M. Li, and Q. Hou, "A modified W-W interatomic potential based on ab initio calculations," ModellingSimul. Mater. Sci. Eng.015004 (2014) 22.

[20] Plimpton, S. "Fast Parallel Algorithms for Short-Range Molecular" Dynamics. J. Comput.Phys. 117, 1–19 (1995).

[21] Egami T., Maeda, K. &Vitek V. "Structural defects in amorphous solids A computer simulation study". Philosophical Magazine A , 41 (6), (1980)883- 901.

[22] A. Stukowski, "Visualization and analysis of atomistic simulation data with OVITO-the Open Visualization Tool", Modell. Simul. Mater. Sci. Eng. 18 (2009) 015012.

[23] Zhe Chen , Laszlo J. Kecskes , Kaigui Zhu , Qiuming Wei , Atomistic simulations of the effect of embedded hydrogen and helium on the tensile properties of monocrystalline and nanocrystalline tungsten, Journal of Nuclear Materials 481 (2016) 190-200.

[24] Frederiksen S L, Jacobsen K W, Schiotz J. Simulations of intergranular fracture in nanocrystalline molybdenum. Acta Mater, 2004, 52: 5019–5029.

[25] Van Swygenhoven H, Derlet PA. Grain-boundary sliding in nanocrystalline fcc metals. Phys. Rev. B 2001;64.

[26] Mohamed FA. Interpretation of nanoscale softening in terms of dislocation-accommodated boundary sliding. Metall Mater Trans A 2007;38A:340.

[27] Schiotz J, Vegge T, Di Tolla FD, Jacobsen KW. Atomic-scale simulations of the mechanical deformation of nanocrystalline metals. Phys. Rev. B 1999;60:11971.

[28] Schiotz J, Di Tolla FD, Jacobsen KW. Softening of nanocrystalline metals at very small grain sizes. Natur 1998;391:561.

[29] Ke M, Hackney SA, Milligan WW, Aifantis EC. Observation and Measurement of Grain Rotation and Plastic Strain in Nanostructured Metal Thin-Films. Nanostruct. Mater. 1995;5:689.

[30] Shan ZW, Stach EA, Wiezorek JMK, Knapp JA, Follstaedt DM, Mao SX. Grain boundary-mediated plasticity in nanocrystalline nickel. Science 2004;305:654.

[31] Legros M, Gianola DS, Hemker KJ. In situ TEM observations of fast grain-boundary motion in stressed. Nanocrystalline aluminum films. Acta Mater. 2008;56:3380.

[32] Rupert TJ, Gianola DS, Gan Y, Hemker KJ. Experimental Observations of Stress-Driven Grain Boundary Migration. Science 2009;326:1686.

[33] Hasnaoui A, Van Swygenhoven H, Derlet PM. Cooperative processes during plastic deformation in nanocrystalline fcc metals: A molecular dynamics simulation. Phys. Rev. B 2002;66:184112.